Motallebi M, Lignos D, Rogers CA (2018), "Behaviour of stiffened extended shear tab connections under gravity induced shear force", Journal of Constructional Steel Research 148: 336-350. DOI/10.1016/j.jcsr.2018.06.011

# Behaviour of Stiffened Extended Shear Tab Connections under Gravity Induced Shear Force

Mohammad Motallebi[1], Dimitrios G. Lignos[2], Colin A. Rogers[3]

[1] Graduate Research Assistant, Department of Civil Engineering and Applied Mechanics, McGill University, Montreal, QC. Email: mohammad.motallebinasrabadi@mail.mcgill.ca

[2] Dimitrios G. Lignos, Associate Professor, School of Architecture, Civil and Environmental Engineering, Swiss Federal Institute of Technology, Lausanne (EPFL), Switzerland, Email: dimitrios.lignos@epfl.ch

[3] Corresponding author
Colin A. Rogers, Associate Professor, Department of Civil Engineering and Applied Mechanics, McGill University, Montreal, QC. Email: colin.rogers@mcgill.ca
817 Sherbrooke Street West
Montreal QC, Canada, H3A 0C3
Tel. 514 398-6449
Fax. 514 398-7361

**ABSTRACT**

Stiffened extended shear tab connections (either in full-depth or partial-depth configurations) are widely used to connect simply supported beams to the web of supporting girders or columns. Full-scale laboratory tests of stiffened extended shear tab connections underscored the differences between their observed and expected design strength calculated according to current design specifications. In particular, the design procedure of such connections neglects the influence of the out-of-plane deformation of the supporting girder web on yielding and inelastic buckling of the shear plate. These are the main governing failure modes for the full-depth configurations of stiffened extended shear tabs, when placed on one side of a supporting girder or column. The research described in this paper aims to develop a better understanding of the load transfer mechanism and failure modes of extended beam-to-girder shear tab connections. The findings are based on finite element (FE) simulations validated with full-scale experiments on beam-to-girder shear tab connections. The influence of girder web flexibility on the behaviour of single-and double-sided shear tabs is assessed. The stiffened portion of the full-depth extended shear tabs yielded due to the interaction of horizontal shear and vertical axial force. Due to the flexibility of the girder web of the single-sided shear tab, its stiffened portion experienced much larger vertical axial force in comparison to that of the double-sided configuration.

**Keywords**: extended shear tab, connection, plate buckling, design, effective eccentricity, finite element simulation

# 1 Introduction

Extended shear tab connections are widely used in steel construction practice due to their ease of fabrication and erection. They consist of a steel plate, which is shop-welded to the supporting girder or column and then bolted to the supported beam in the field. The increased shear tab length allows the beam to be connected to the girder web without coping the beam's flanges (Fig. 1). The shear plate may be welded to the girder web alone, i.e. unstiffened configuration (Fig. 1a), or may be connected either to the top flange, i.e. partial-depth stiffened configuration (Fig. 1b) or to both the top and bottom flanges, i.e. full-depth stiffened configuration (Fig. 1c). Similarly, connection to the minor axis of a W-shape column can benefit from the use of an extended shear tab.

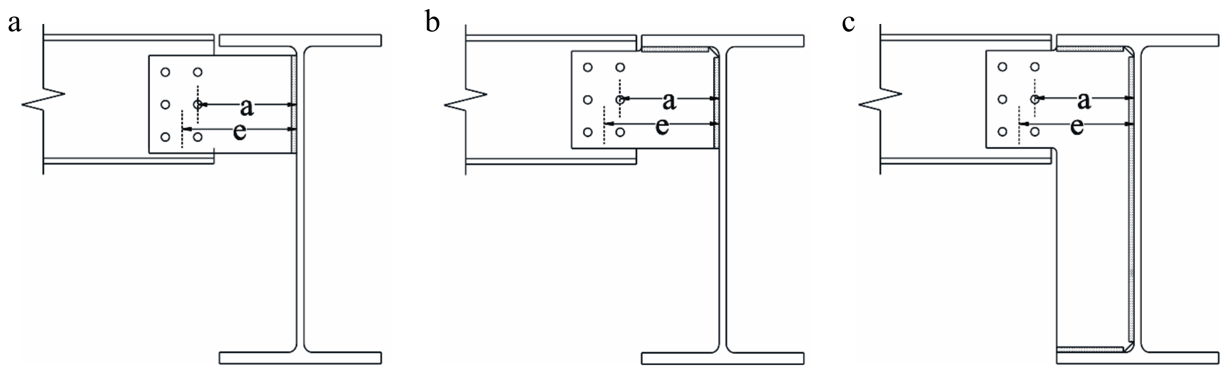


Fig. 1. Extended beam-to-girder shear tab connections: (a) partial-depth unstiffened, (b) partial-depth stiffened, (c) full-depth stiffened

The potential failure modes of unstiffened extended shear tab connections are summarized in the 15h Edition of the AISC Steel Construction Manual [1]. The plate thickness and the weld throat are proportioned to develop plate yielding prior to bolt shear and weld tearing such that a stable behaviour can be achieved for the imposed loading. The 15th Edition of the AISC Steel Construction Manual [1] uses the rectangular plate buckling model [2,3] to account for flexural buckling of the shear plate, while the 14th Edition of the AISC Steel Construction Manual [4] implements equations corresponding to the flexural buckling resistance of a doubly coped beam [5-6].

The AISC design method [1] was originally developed for unstiffened extended shear tabs connected to rigid supports. The same method was further applied to unstiffened extended shear tabs connected to flexible supports by considering the out-of-plane deformation of the supporting element's web (either girder or column) as a serviceability issue for the supported beam [7]. The AISC design method was not originally developed for use with the partial-depth or full-depth stiffened extended shear tab. The shear tab in this case, may impose higher rotational demands to the supporting member (girder or column), which are typically not considered in frame analysis. This raises concern about the desirability of using stiffened extended shear tabs [8]. Nonetheless, practicing structural engineers do use stiffened extended shear tabs, typically, when an increase in the thickness of the shear plate is not a reasonable option to address the need to stabilize either the beam or the shear plate itself. The stiffened detail may be chosen because an upper limit is placed on the thickness of the shear plate to ensure its yielding prior to shear fracture of the bolts. Hence, an increase in thickness of the shear plate to improve its stability may not be permitted.

Further, specific to a beam-to-column connection, the column may also need continuity plates if there exists a fully restrained beam-to-column moment connection in the perpendicular direction. This allows for the possibility of attaching the extended shear tab to these plates as a lateral stability bracing. As well, even when continuity plates are not required, horizontal stabilizer plates may be added to laterally support the extended shear tab attached in the minor direction of a W-shape column. Moreover, if the supporting members are part of the primary lateral load-resisting system, their behaviour under gravity and lateral loads may be adversely affected by a potential out-of-plane deformation of the respective columns and/or girders. This may be particularly concerning when deep members are utilized in the lateral load resisting system [9]. Stiffened shear tab connections may also be chosen for this reason. Given these situations, in which extended shear tabs are stiffened, there exists the need to better understand their behaviour under load, and ultimately to ascertain whether existing design methods are appropriate. As a first step, the design method found in the AISC Manual [1] can be utilized to identify the potential failure modes of these shear tab connections.

In the design of extended shear tabs the current AISC Manual [1] suggests the inflection point to be located at the face of the supporting member, i.e. the girder web in this case (Fig. 2a). The design shear force and flexural moment for the bolt group (Figs. 2b and 3a) are the shear force at the beam end (R) and the resultant eccentric moment (M=R × e), respectively. Furthermore, the vertical weld line, which connects the shear plate to the girder web (or the column web as shown in Fig. 3a), is designed to resist the shear force (R) alone. The horizontal weld lines, that connect the shear plate to the girder flanges (the stabilizer plates in Fig. 3a), are not considered as load carrying welds; as such, they are detailed having a minimum size. Of note, Figs. 2b and 3a show the symmetric configuration where the centreline of the supported beams is located midway between the girder flanges (the two stabilizer plates in Fig 3a). This configuration may not be applicable if a supported beam is connected to a deeper supporting girder (Fig. 2c). Further, the symmetric configuration may not be applicable in the presence of continuity plates of a fully restrained moment connection joining a deeper beam to the column in the orthogonal direction (Fig. 3b).

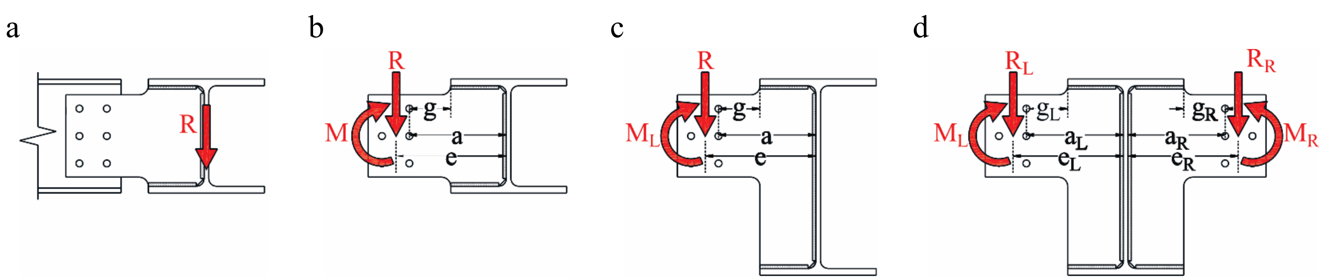


Fig. 2. Full-depth stiffened extended beam-to-girder shear tab: (a) location of inflection point, (b) single-sided (the beam and girder have the same depth), (c) single-sided, (d) double-sided

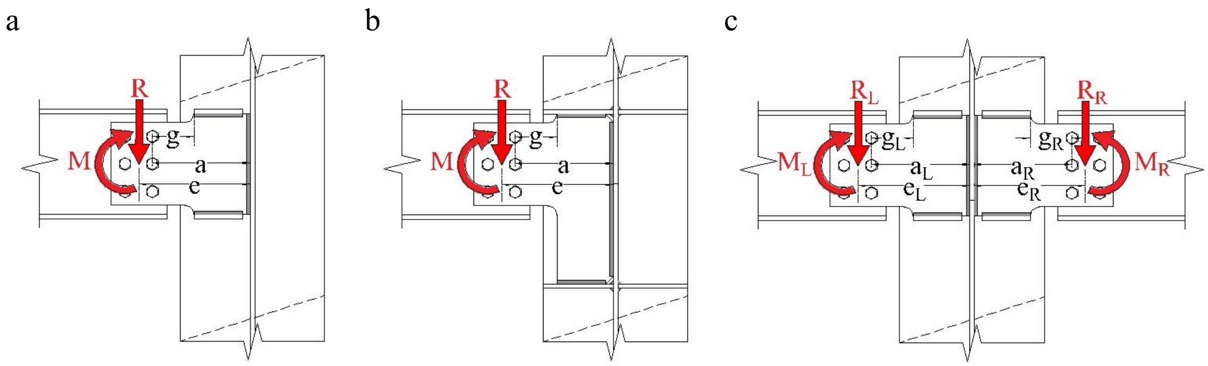

Fig. 3. Full-depth stiffened extended beam-to-column shear tab: (a) single-sided, (b) single-sided with continuity plates, (c) double-sided

For a girder or column, which supports a beam on both sides (Figs. 2d and 3c), each connection is designed for its corresponding shear force ($R_R$ and $R_L$) and a portion of the net flexural moment ($M_R$-$M_L$=$R_R$×$e_R$ - $R_L$×$e_L$) determined based on the engineer's judgement [1]. For the design of other connection elements, i.e. the shear plate and stabilizer plates, the current AISC Manual gives no explicit recommendations.

It is often the case that the design procedure of stiffened beam-to-girder shear tabs follows that of the unstiffened ones; the bolt group and the gross section of the plate are designed for the connection shear force (R) and the resultant eccentric bending moment (R × e and R × a, respectively). This leads to either bolt shear fracture or yielding of the extended portion of the shear plate as the governing failure mode of the stiffened shear tab connection if the current AISC design approach [1] is followed. However, this is not consistent with the observed behaviour of such connections from laboratory tests [10-12].

Findings from past experimental and finite element studies [10-13] reveal that bolt shear fracture is not deemed to be critical in the context of the connection configurations that were evaluated. Plate buckling is the governing failure mode for stiffened full-depth configurations of either beam-to-girder [10] or beam-to-column shear tab connections [11, 12]. Notably, in stiffened extended beam-to-girder shear tabs with a partial-depth shear plate, shear plate yielding and twisting were the governing failure modes [10, 13]. Although the girder web mechanism was evident, it was a secondary failure mode that mostly occurred in deep connections, i.e. shear tab connections with a single vertical line of six or more bolts [10,13].

In order to improve the current design provisions for full-depth stiffened extended shear tabs, Fortney and Thornton [14] recommended that the distance between the bolt line and the toe of a stabilizer plate should be used as the bolt group eccentricity for the design of extended shear tabs with stabilizer plates. Neither published laboratory tests nor finite element analyses were provided to fully explain this recommendation. Although the design calculations based on the aforementioned eccentricity result in a higher prediction for the bolt shear strength, they still overestimate the shear plate buckling strength, which is the governing failure mode observed in laboratory tests [10-12].

The test results of extended beam-to-girder shear tabs are limited to a few configurations with a single vertical row of bolts, although shear tabs with multiple bolt lines are common in current steel construction practice. Multiple bolt lines may decrease the shear plate buckling strength because the shear plate is loaded farther from its support, the weld line. Furthermore, most of the experimental studies on stiffened beam-to-column shear tabs [12] were limited to the configuration similar to that shown in Fig. 3a. Nevertheless, this configuration would need to be modified if continuity plates were incorporated into a fully restrained beam-to-column connection (Fig. 3b), resulting in a full-depth stiffened shear tab connection. As such, conflicting opinions exist regarding the design of stiffened extended shear tabs, and the definition of the eccentric loading.

To further our understanding on how unstiffened and stiffened extended shear tab connections behave under gravity-induced shear forces, a research program was carried out at McGill University. Full-scale laboratory tests of extended and various other shear tabs were first conducted [15-22]. These test results allow for a better comprehension of the nonlinear behaviour of shear tab connections under monotonic loading. The testing program was complemented with detailed finite element (FE) simulations. Several parameters were interrogated to further our understanding of the behaviour of extended shear tab beam-to-girder connections. This paper presents the findings from the corroborating finite element analysis of the research program for two specific beam-to-girder extended stiffened shear tab connections. The main objective was to gain insight into the differences in load transfer mechanism of single- and double-sided stiffened full-depth extended shear tabs.

## 2 Brief description of full-scale laboratory testing at McGill University

Fifty-five full-scale laboratory tests were conducted at McGill University [15-22] to characterize and further understand the behaviour of shear tab connections, including both standard and extended configurations, beam-to-column and beam-to-girder arrangements, as well as bolted and welded details. The connection configurations reflect the current practice in North America. Among these tests, two specimens of stiffened full-depth extended beam-to-girder shear tabs with two vertical rows of three bolts (Figs. 4a and 4b) were selected to develop finite element models to further our understanding regarding their behaviour under gravity-induced shear forces; BG3-2-10-F [19] and BG3-2-13-F [20]. These specimens were nominally identical except for the thickness of the respective shear plate; the shear plate was 10 mm thick for Specimen BG3-2-10-F, and 13 mm for BG3-2-13-F. In particular, the thickness of the shear plate of Specimen BG3-2-13-F was increased to satisfy the current compactness criteria for the stiffener of a plate girder as per CSA S16 [23] ($200/\sqrt{F_y}$). This corresponds to the AISC 360 [2] width-to-thickness ratio for unstiffened elements subjected to axial compression (Table B4.1a, $0.45\sqrt{E/F_y}$). Of note, the shear plate compactness is not part of the AISC shear tab design method [1]; this method addresses unstiffened shear tab connections where plate local buckling is not a concern.

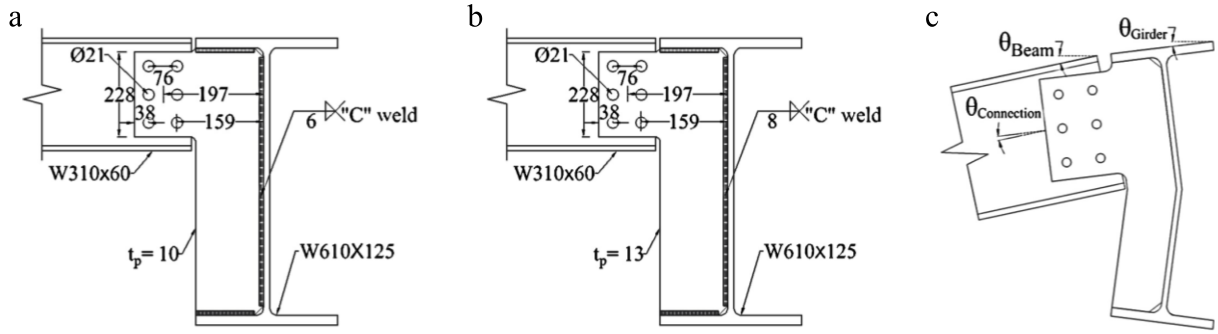


Fig. 4. Laboratory tests of beam-to-girder shear tabs: (a) details of Specimen BG3-2-10-F, (b) details of Specimen BG3-2-13-F, (c) measured rotations of specimens (dimensions in mm)

The beam and girder were fabricated from ASTM A992 Grade 50 steel [24], while the shear plates were made of ASTM A572 Grade 50 steel [25]; for both grades the nominal $F_y$=345 MPa and $F_u$=448 MPa. To attach the shear tab to the supporting girder, an E71T (nominal $F_u$=490 MPa) electrode was used in a flux-cored arc welding process with additional shielding gas ($CO_2$) to provide a fillet weld on both sides of the plate. Each beam was snug tightened to the shear tab using 19 mm (3/4 in.) ASTM F3125 Grade A325 bolts [26] in standard size holes (20.6 mm (13/16 in.)). The test setup (Fig. 5) consisted of a 12 MN and a 445 kN hydraulic actuator, a lateral bracing system for the steel beam, and supporting elements for the girder. The 12 MN actuator, located near the shear tab connection, developed the main shear force in the connection. The 445 kN actuator, placed at the far end of the beam, facilitated the vertical displacement control of the beam tip, as well as the connection rotation. The relative rotation between the beam and the girder was defined as the connection rotation (Fig. 4c). The lateral bracing system was installed to restrict the lateral displacement of the beam, without affecting its vertical displacement. This test setup, to apply simultaneous shear force and rotation to the connection, is based on that used in prior research of shear tab connections [27].

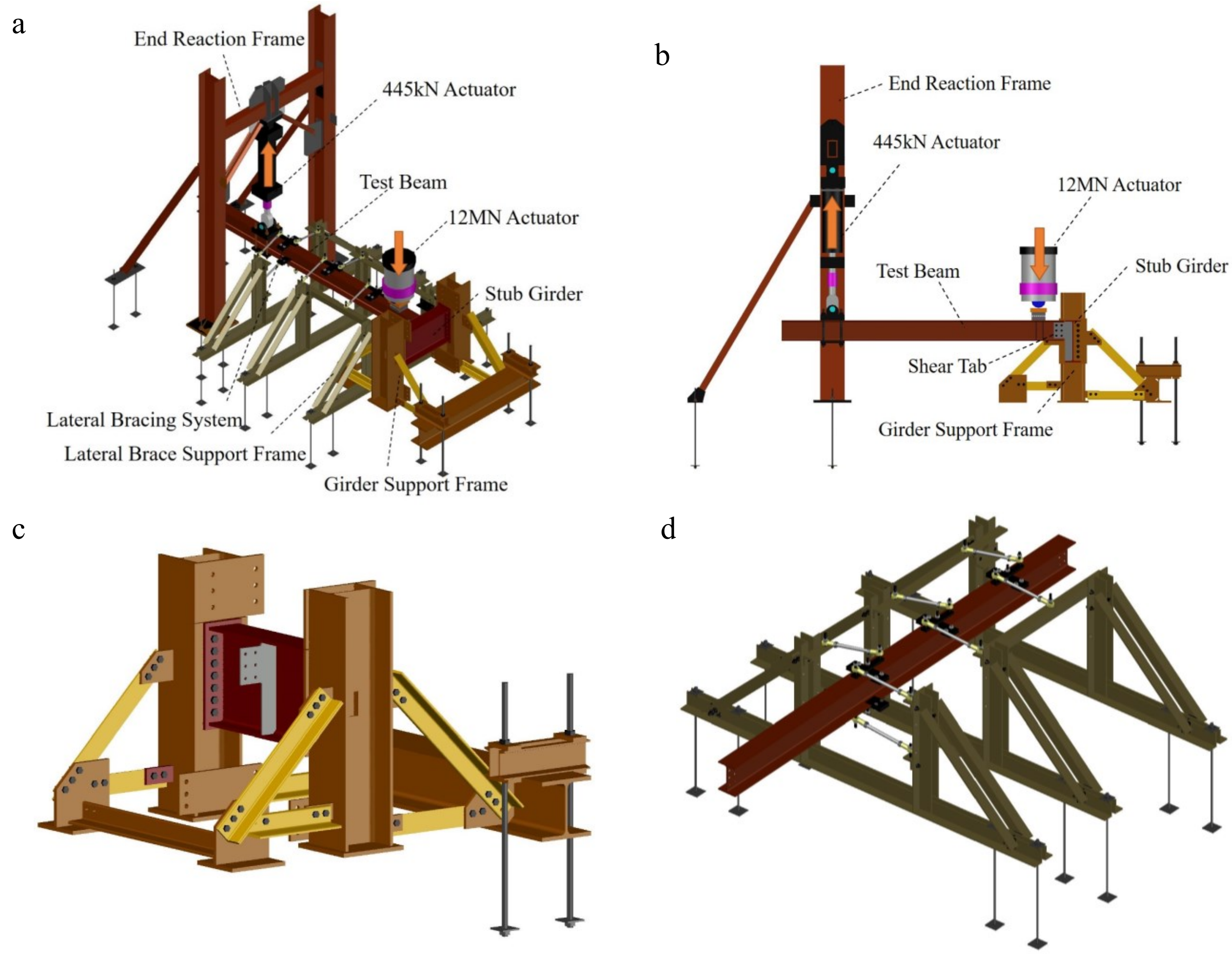


Fig. 5. Laboratory tests of beam-to-girder shear tabs: (a) overall test setup, (b) elevation view (lateral bracing system was not shown for clarity), (c) close-up view of the shear tab connection, girder, and its supporting frame, (d) view of the test beam and its lateral bracing system

Linear Variable Differential Transformers (LVDTs) were installed to measure the out-of-plane deformation of the beam, as well as that of the shear plate and of the girder web (Fig. 6). In-plane rotation of the beam and girder were measured using inclinometers (Fig. 6). A complete description of the test programs can be found in [19, 20].

On the basis of the current AISC design procedure [1], Table 1 contains a summary of the calculated connection strengths corresponding to the probable failure modes. The contact between the shear plate and girder flanges was ignored; the shear plate was designed as would be done for an unstiffened shear tab. Hence, the distance between the girder web and the interior bolt line (the *a* distance) was conservatively considered to be the unbraced length of the shear plate. Of note, this method resulted in a more conservative prediction for the shear plate buckling as compared to Fortney and Thornton's recommendation [14] for the connection eccentricity.

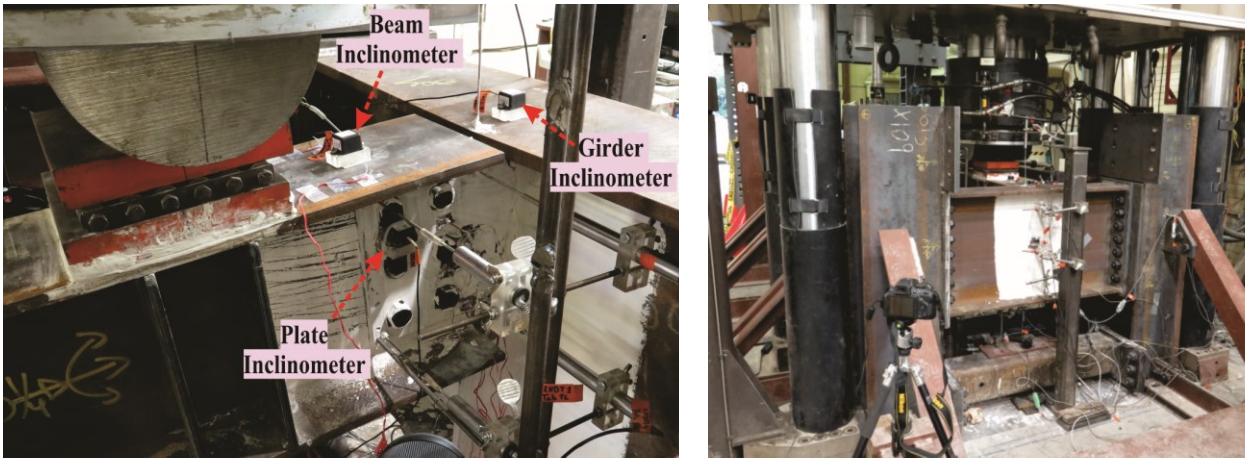


Fig. 6. Laboratory test of beam-to-girder shear tab specimen BG3-2-13-F

Table 1 AISC predicted strength of shear tab test specimens

| | BG3-2-10-F | | | BG3-2-13-F | | |
|---|---|---|---|---|---|---|
| Failure mode | Design strength (kN) | Expected strength[1] (kN) | Expected strength[2] (kN) | Design strength (kN) | Expected strength[1] (kN) | Expected strength[3] (kN) |
| Flexural and shear yielding of shear plate | 214 | 255 | 307 | 281 | 334 | 390 |
| Shear yielding of shear plate | 450 | 495 | 596 | 591 | 650 | 758 |
| Bolt bearing | 191 | 280 | 305 | 191 | 280 | 290 |
| Buckling of shear plate | 243 | 297 | 357 | 319 | 390 | 455 |
| Rupture at net section of shear plate | 318 | 509 | 496 | 417 | 667 | 654 |
| Bolt shear | 182 | 270 | 270 | 182 | 270 | 270 |
| Weld tearing | 1035 | 1380 | 1380 | 1294 | 1725 | 1725 |

[1]Expected strength based on probable material properties i.e.$R_yF_y$ (1.1 $F_y$) and $R_TF_u$ (1.2 $F_u$) for steel plates [27]
[2]Expected strength based on measured material properties i.e $F_y$=456MPa and $F_y$=525MPa for 10mm plate
[3]Expected strength based on measured material properties i.e $F_y$=442MPa and $F_y$=527MPa for 13mm plate

The buckling strength of the shear plate was calculated using two methods: rectangular plate buckling [1] and buckling of the double coped beam [4]. Both methods predicted that buckling would not prevent the shear plate from reaching its nominal plastic flexural capacity ($M_p=F_yZ_p$). In addition to the nominal and expected material properties, the measured properties (coupon tests [19, 20]) of the steel beam, girder and plate were used to conduct these AISC-based calculations, whereas the nominal properties of the bolts and welds were relied on in this process.

Regarding the shear plate-to-girder weld, its size meets the AISC minimum requirement ( $a_w \geq 5/8t_p$ ), and the reported weld tearing strength is the concentric shear capacity of the vertical weld line. To ensure yielding of the shear plate in advance of bolt shear fracture, the AISC requirement for maximum shear plate thickness was controlled using the nominal yield stress of the shear plate, as well as its expected and measured material properties. Although both configurations meet this requirement, the bolt shear fracture was predicted as the governing failure mode in all cases, other than for calculations based on the expected material properties of Specimen BG3-2-10-F.

Referring to Fig. 7a, both specimens showed very ductile response; these tests were terminated due to binding between the beam's bottom flange and the shear plate. The binding took place at 271 kN (0.073 rad) and 520 kN (0.129 rad) for Specimens BG3-2-10-F and BG3-2-13-F, respectively. However, it should be noted that it would be imprudent to rely on these ultimate shear resistances in the design of extended shear tabs because the large rotation, needed to develop this shear force, would be detrimental to the serviceability of the supported beam.

The yielding and out-of-plane deformation of the girder web and the stiffened section of the shear tab (Figs. 7b and 7c), which was confined between the girder web and flanges, were observed as failure modes. The stiffness of specimen BG3-2-10-F degraded significantly at 221 kN shear force (82% of the connection expected strength, i.e., 270 kN), while the stiffness of specimen BG3-2-13-F decreased at 390kN shear force (144% of the connection expected strength, i.e., 270 kN). Contrary to the design predictions, bolt shear failure did not occur in any of the full-scale tests, nor did the bolts exhibit damage. It was observed that the inflection point formed away from the girder web and close to the centre of the bolt group. As such, the bolt group eccentricity was much smaller than the AISC assumption, the distance between the weld line and the centre of the bolt group (the geometric eccentricity). Further discussion of this aspect is provided in Section 5.2.

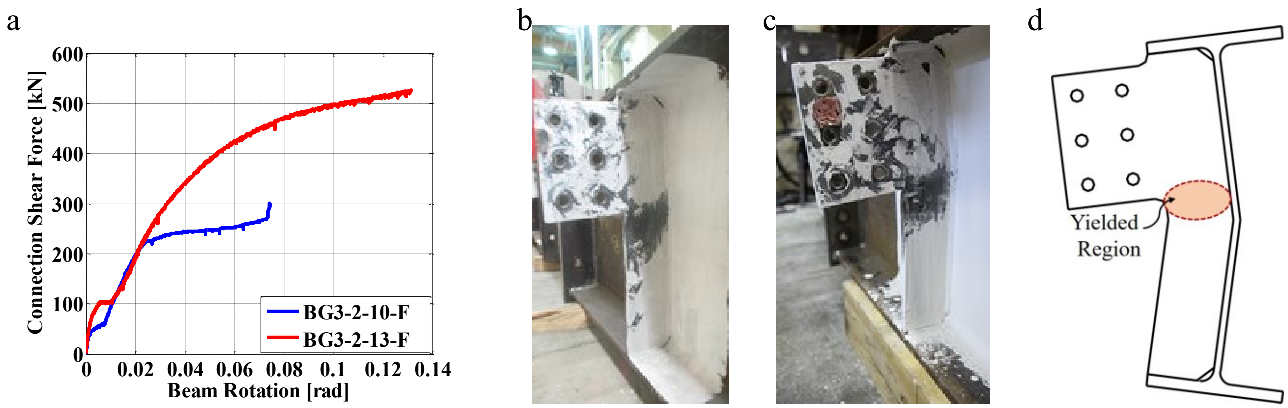


Fig. 7. Test results: (a) shear force versus Beam rotation, (b) deformed shape of specimen BG3-2-10-F, (c) deformed shape of specimen BG3-2-13-F, (d) girder web mechanism

## 3 Finite element simulation of extended beam-to-girder shear tab connections

The finite element (FE) models were developed in the commercial software ABAQUS-6.11-3 [29] to obtain a better understanding of the behaviour of extended beam-to-girder shear tab connections with full-depth stiffeners under gravity-induced shear forces. The main features of the FE models (Fig. 8) were chosen to be representative of those seen in the laboratory experiments; including geometry, boundary conditions, material properties, element size and element type, contacts and interactions, and the imposed loading protocol. The employed material properties were defined based on the engineering stress-strain curves obtained from tensile coupon tests, directly extracted from the various components of the tested subassemblies. These were then converted to true stress-strain curves. The material properties for the bolt and welds were defined based on typical stress-strain curves, obtained from Kulak et al. [30] and Gomez et al. [31], respectively, which were scaled to meet the minimum specified values. Of note, all constitutive material models were defined up to the ultimate strain.

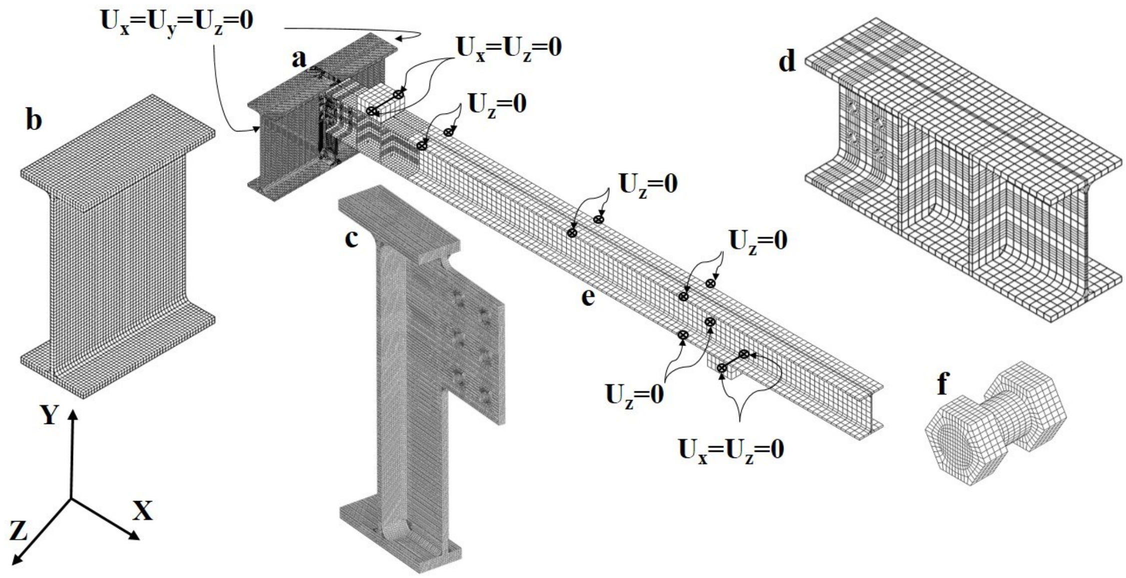


Fig. 8. Finite element model specifics: (a) overall model, (b) girder mesh (typical element size of 10 mm), (c) shear plate mesh (typical element size of 3 mm), (d) mesh of the beam in the vicinity of connection (typical element size of 20 mm), (e) beam mesh (typical element size of 40 mm), (f) bolt mesh (Typical element size of 1.5 mm)

First-order fully-integrated 3D solid elements were utilized to mesh the FE models of the shear tabs (Fig. 8). The element size was determined based on a mesh sensitivity analysis. The stub columns (Fig. 5c) were replaced by idealized fixed boundary conditions to create a computationally efficient FE model. To simulate the lateral braces (Fig. 5d) of the beams, the lateral displacement of the beam flanges at the locations of the braces was restricted. The loading protocol was simulated by applying the displacements of the two actuators, recorded during the tests, to the centerline of the load cubes, while the horizontal ($U_x$) and out-of-plane deformation ($U_z$) of the load cubes' centerline were prevented. To allow transmission of tangential force between the components in contact, a friction coefficient of 0.3 was used for all surface-to-surface contact pairs, except those between the load cubes and the flanges of the beam where frictionless interaction was defined. The normal behaviour of contacts, allowing separation after closure, was defined using a hard contact formulation with a penalty constraint enforcement method. Furthermore, to trigger possible local instabilities of the shear tab connection, local imperfections were introduced into the shear plate and girder. In order to define the local imperfections, the nodal coordinates of the shear plate and girder were modified by scaling appropriate buckling mode shapes, obtained from eigenvalue buckling analysis. These local imperfections were proportioned to the limits of manufacturing tolerances for the web of W-sections (d/150) [32-34]. This approach was found to be satisfactory in prior FE studies by Elkady and Lignos [35] to simulate the onset of local and/or member geometric instabilities.

### 3.1 Comparison of numerical and experimental results

In order to evaluate the accuracy of the numerical models, their predictions were compared to test results. Among others, the developed shear force of the connection and the girder web out-of-plane deformation were chosen as the primary model verification criteria as shown in Fig. 9.

Referring to Figs. 9a to 9d, the predicted shear force response deviated from the test measurements only in the initial increments of the applied loading. This discrepancy is due to uncertainties related to the contact between the bolt shanks and the bolt holes for each specimen due to fabrication tolerances and installation of the respective test specimens. The shear tab connections were snug-tightened, hence, bearing between the bolt shanks and bolt holes transferred the shear force between the beam and the shear plate. Further, the initial position of each bolt in its hole was not controlled during testing, leading to an unknown slip before contact bearing. In the FE model, the bolts were consistently placed at the bolt hole centre, resulting in an initial 0.8 mm (1/32 in.) gap around the entire perimeter of the bolt shanks, which matches the fabrication tolerance of standard 21 mm (13/16 in.) holes. To prevent rigid body motion of the beam, and consequently to overcome issues with numerical convergence of the FE model, a small amount of bolt pretension, i.e. 50 MPa, was applied as suggested in prior related studies [36].

Figure 9f suggests that the FE models predict reasonably well the out-of-plane deformations of the girder web of connection BG3-2-13-F. For shear tab connection BG3-2-10-F (Fig. 9e), the girder web out-of-plane deformation was not accurately measured due to the malfunction of one of the LVDTs (LVDT6).

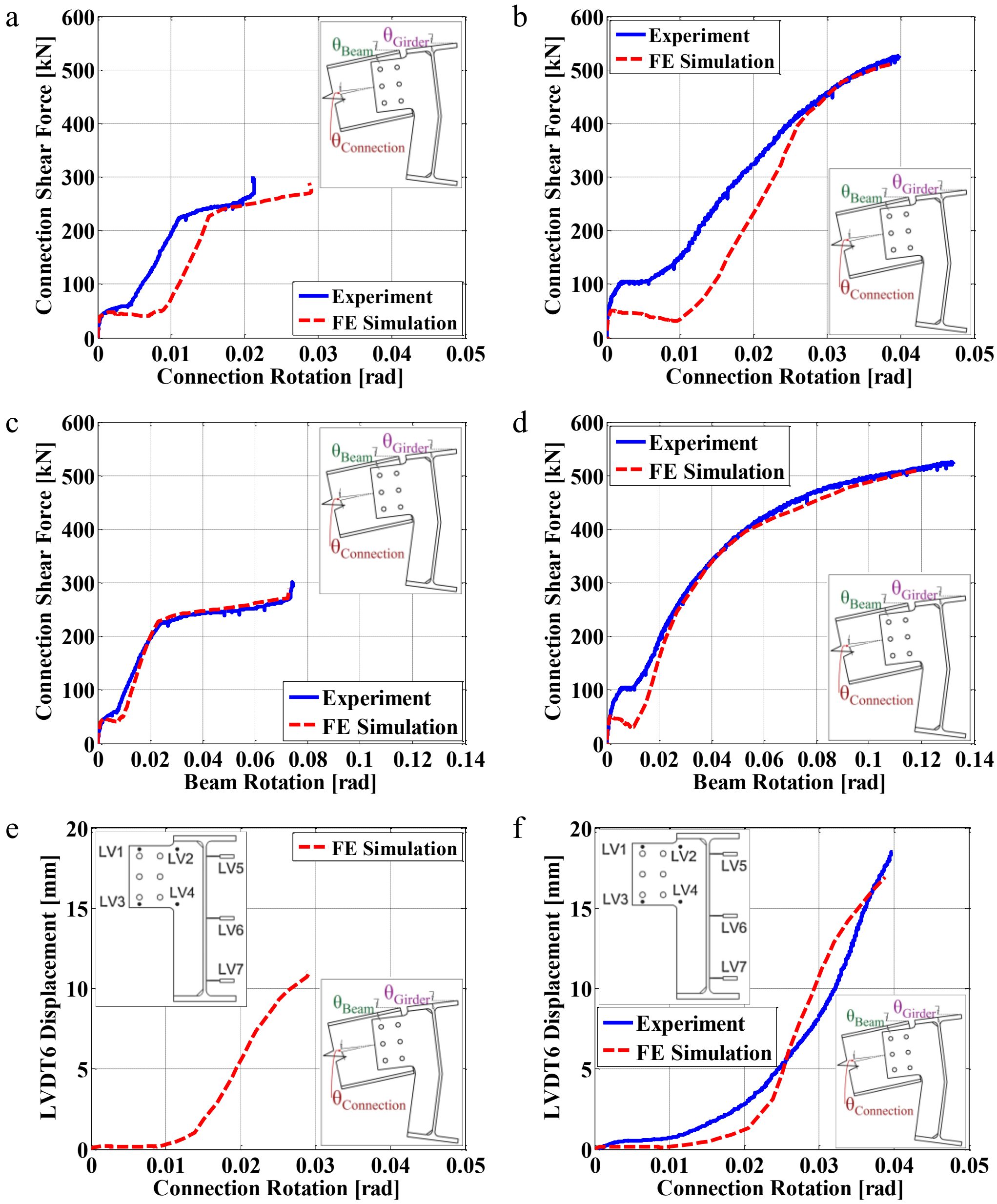


Fig. 9. Numerical model verification: (a) shear force versus connection rotation of BG3-2-10-F, (b) shear force versus connection rotation of BG3-2-13-F, (c) shear force versus beam rotation of BG3-2-10-F, (d) shear force versus beam rotation of BG3-2-13-F, (e) girder web out-of-plane deformation versus connection rotation of BG3-2-10-F, (f) girder web out-of-plane deformation versus connection rotation of BG3-2-13-F

## 4 Observed failure modes of extended beam-to-girder shear tab connections

It is rather challenging to observe the individual failure modes of shear tab connections addressed in the AISC Steel Construction Manual [1] by solely conducting physical experiments. This is due to the failure mode coupling after the connection exhibits inelastic behaviour. As such, a numerical study was conducted in which the strength of the connection components (beam, shear plate, bolts, and girder) were determined. The calibrated FE models for shear tab configurations BG3-2-10-F and BG3-2-13-F served as baseline models.

The features and the targeted behavioural aspects associated with each individual FE model are presented in Table 2, and are further discussed in Sections 4.1 and 4.2. In the FE-E model, all the material properties were assumed to be elastic such that the elastic stiffness of the shear tab connection could be computed. The FE models with damageable components advanced our understanding in the load redistribution due to material nonlinearity and/or geometric instabilities occurring within a connection. Both single- and double-sided shear tabs were investigated.

Table 2-Features and targeted behavioural aspects of FE models

| Model Notation | Features | Behavioural Aspect |
|---|---|---|
| FE-E | All components elastic | Elastic stiffness and elastic buckling strength |
| FE-E-G | All components elastic except girder | Out-of-plane bending capacity of girder web |
| FE-E-Be | All components elastic except beam | Effect of beam yielding on response of connection |
| FE-E-Bo | All components elastic except bolts | Shear capacity of bolt group |
| FE-E-SH | All components elastic except shear plate | Strength of shear plate |
| FE-Pl | Yieldable material properties assigned to all components | Strength of connection and interactions between failure modes |
| FE-Pl-Imp | Yieldable material properties assigned to all components. Initial imperfections assigned to trigger buckling of shear tab | Effect of initial imperfection on behaviour of shear tab |

## 4.1 Single-sided shear tabs

The results of the numerical FE study for shear tab connections BG3-2-10-F and BG3-2-13-F are illustrated in Figs. 10 and 11, respectively. The shear force of BG3-2-10-F is presented versus the connection rotation and the beam rotation in Figs. 10a and 10b, respectively. Displacements of LVDT

4 and LVDT 6 (Figs. 9e and 9f) are presented versus the connection rotation in Figs. 10c and 10d, respectively.

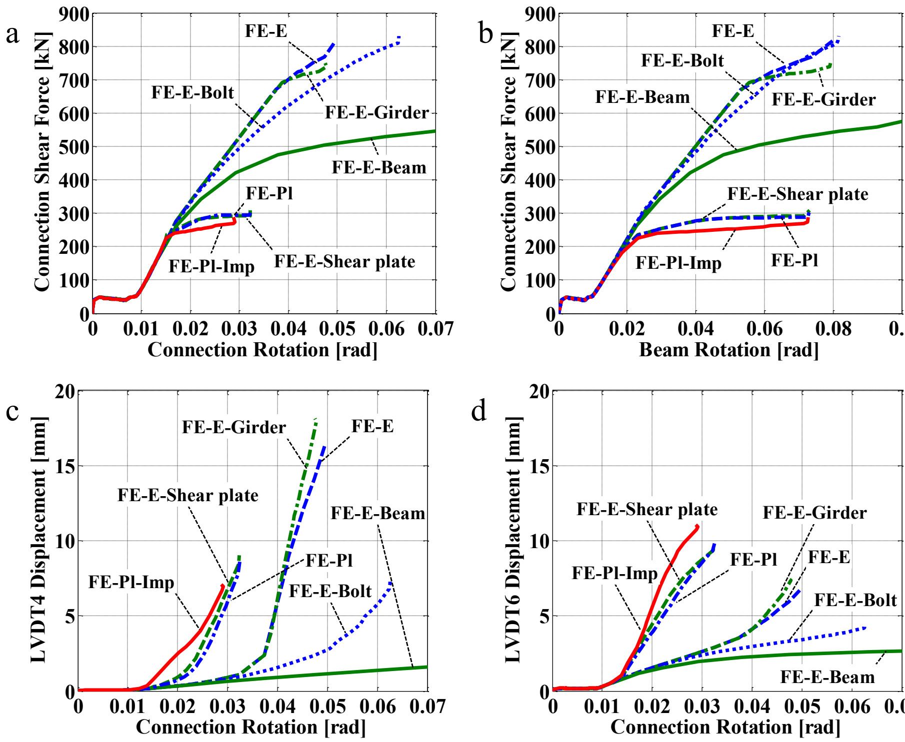


Fig. 10. Predictions of numerical models for shear tab connection BG3-2-10-F

Referring to Figs. 10 and 11, the FE-E model suggests a near bilinear response. In general, a significant loss in stiffness is identified when the slope of the curve representing the out-of-plane deformation of the shear plate (LVDT4) versus connection rotation (Fig. 10c) exhibits a sudden increase. This stiffness change is associated with the bifurcation point due to elastic buckling. Figures 10d and 11d show a substantial increase in the girder web out-of-plane deformation slope (LVDT6) following elastic buckling of the shear plate. A comparison between the FE-E model and the model with a yieldable girder (FE-E-G), demonstrated that their response was approximately identical prior to the onset of girder web yielding. For the slender shear tab (BG3-2-10-F), Fig. 10a shows that the connection with a yieldable girder lost its stiffness and reached its capping strength soon after the shear plate buckled. The strength plateau of the FE-E-G model was attributed to yielding of a large part of the girder web, due to the out-of-plane bending, and formation of a mechanism in the girder web (Fig. 7d).

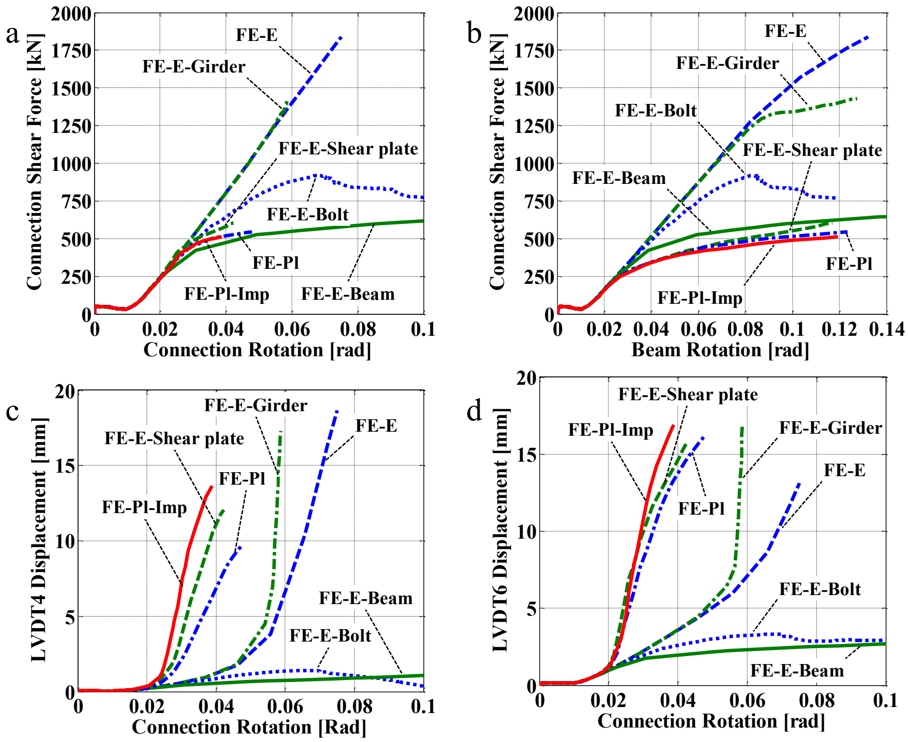

Fig. 11. Predictions of numerical models for shear tab connection BG3-2-13-F

In contrast, Fig. 11a shows that the FE-E-G model of the compact shear tab (BG3-2-13-F) lost its stiffness prior to the shear plate elastic buckling due to the shear yielding of the bottom part of the girder web.

Figures 10 and 11 demonstrate the great dependency of the connection response on the yielding of the shear plate. The yieldable shear plate, i.e. shear plate of models FE-E-SH, FE-Pl, and FE-Pl-Imp, began to yield at the lower re-entrant corner (Figs. 12a and 12b), while its out-of-plane deformation was negligible. As the shear force increased, the yielding propagated to the stiffened part of the shear plate, while the out-of-plane deformation of the plate increased. Referring to Fig. 10a, the slender shear plate (BG3-2-10-F) lost its stiffness when yielding propagated through the full width of its stiffened portion (Figs. 12c and 12d). In contrast, Fig. 11a shows that the compact shear tab (BG3-2-13-F) was able to continue resisting shear after yielding of the stiffener, although its stiffness slightly decreased at this point.

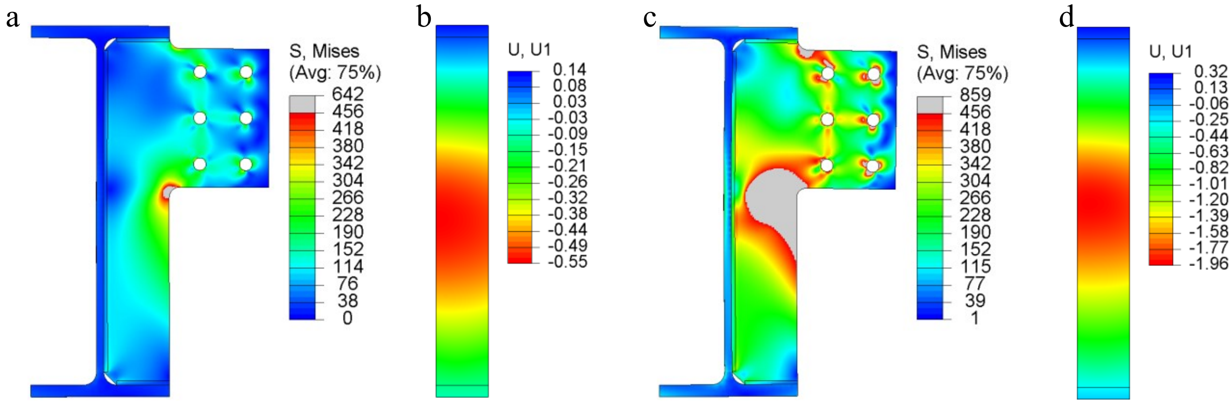

Fig. 12. Prediction of model FE-E-SH of BG3-2-10-F for: (a) stress of shear plate at θ=0.0115 rad, (b) out-of-plane deformation of girder web at θ= 0.0115 rad, (c) stress of shear plate at θ= 0.0155 rad, (d) out-of-plane deformation of girder web at θ= 0.0155 rad (The grey colour represents yielded regions)

In comparison to the FE-E-SH model, the girder web of the FE-Pl model began to yield soon after yielding of the stiffener, which resulted in a slightly lower shear force at the end of the analysis. Referring to Figs. 10 and 11, the shear plate and the girder web of the model incorporating imperfections experienced a larger out-of-plane deformation at the same level of shear force as compared with model FE-Pl. In comparison to model FE-Pl, this imperfection resulted in a slight decrease in the capping strength (9% and 5% for BG3-2-10-F and BG3-2-13-F, respectively) of the model FE-Pl-Imp.

### 4.2 Double-sided shear tabs

As presented in the Section 4.1, the girder web out-of-plane deformation influenced the failure mode of single-sided shear tabs. However, the contribution of this failure mode may be insignificant for double-sided shear tab connections, where two beams, one framed to each side of the girder, counterbalance the moments of each other. To investigate the behaviour of double-sided shear tabs, a series of FE analyses, as described in Table 2, was conducted for shear tab connections BG3-2-10-F and BG3-2-13-F. To decrease computational costs, symmetric boundary conditions were implemented along the girder axis; a beam and half of a girder section were included in these FE models. The FE results for connections BG3-2-10-F and BG3-2-13-F are presented in Fig. 13.

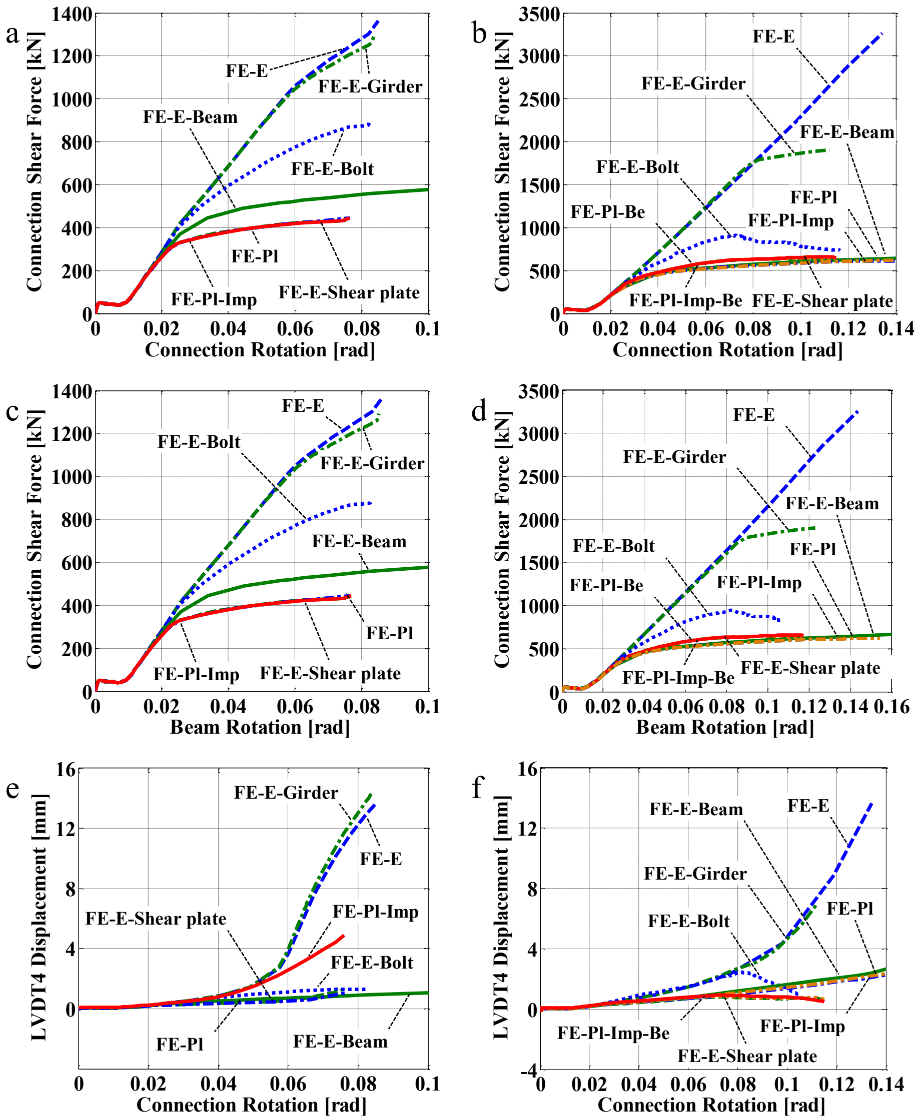


Fig. 13. FE models for double-sided shear tabs: (a) prediction for shear force versus connection rotation of BG3-2-10-F, (b) prediction for shear force versus connection rotation of BG3-2-13-F, (c) prediction for shear force versus beam rotation of BG3-2-10-F, (d) prediction for shear force versus beam rotation of BG3-2-13-F, (e) prediction for out-of -plane deformation of shear plate versus connection rotation of BG3-2-10-F, (f) prediction for out-of -plane deformation of shear plate versus connection rotation of BG3-2-13-F

Referring to Figs. 13a and 13b, the bifurcation point due to elastic buckling of the shear plate was observed in the slender shear tab (BG3-2-10-F), while the stiffness of the connection with a compact shear plate (BG3-2-13-F) remained constant, even though its shear plate experienced large out-of-plane deformations. The response of the FE model with a yieldable girder was identical to the elastic model up to the yielding of the girder web. The out-of-plane deformation of the girder web was restrained, which led to yielding of the girder web due to the applied shear force. This girder web yielding mechanism is distinct from the yielding mechanism of the single-sided configuration, in which the yielding of the girder's web began mainly due to its out-of-plane bending. For the numerical model containing a yieldable shear plate, the onset of yielding occurred at the re-entrant corner of the shear plate when its out-of-plane deformation was negligible. Unlike the single-sided connections, the yielding propagated along the bolt line instead of through the stiffened part of the shear plate. The total height of the shear plate along the bolt line, closest to the girder, yielded and the connection stiffness decreased significantly at this point.

Figure 13 shows that the predictions of the FE-Pl and FE-Pl-Imp models of BG3-2-10-F were close to those of the model with a yieldable shear plate. This occurred because the corresponding shear force demand was not sufficient to develop yielding in the girder web, as shown in Fig. 14. However, after yielding of the full depth of the shear plate along the interior bolt line of model FE-Pl-Imp (Fig. 14a), yielding propagated from the stiffened portion of the shear plate (Fig. 14c), and the out-of-plane deformation of the plate increased. Referring to Fig. 13b, the results of models FE-Pl and FE-Pl-Imp of BG3-2-13-F deviated from the results of the model FE-E-SH due to the yielding of the beam's web along the net section of the vertical row of bolts, farthest from the girder. As the main purpose of this study was to investigate the behaviour of the shear tab connection, the effect of beam yielding was prevented from dominating the results of the numerical model FE-Pl-Be by assigning elastic material properties to the beam, while the other components were defined to experience yielding. Figure 13b shows that the results of this model and model FE-Pl-Imp-Be, were identical to the model with a yieldable shear tab because the level of shear force was not sufficient to initiate yielding of the girder web.

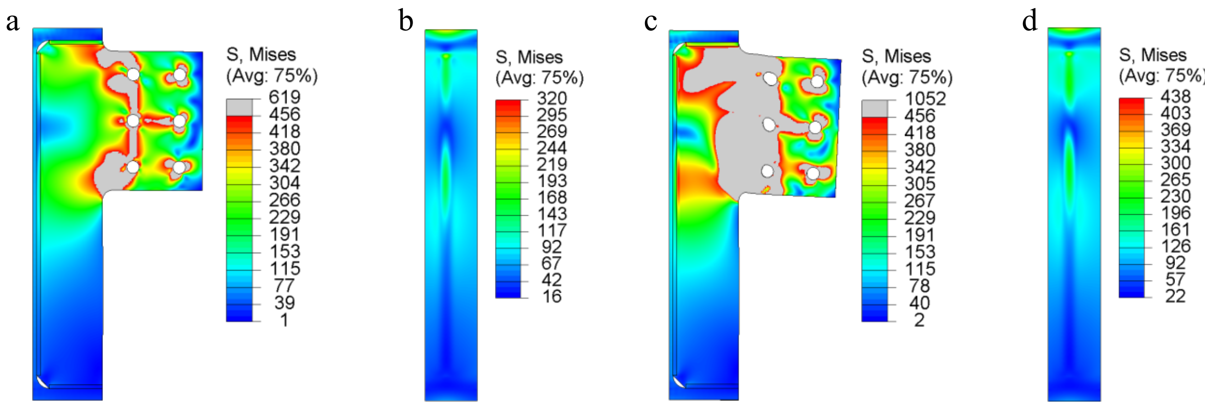


Fig. 14. Prediction of model FE-Pl-Imp of BG3-2-10-F for stress of: (a) shear plate at θ=0.0223 rad, (b) girder web at θ=0.0223 rad, (c) shear plate at θ=0.0603 rad, (d) girder web at θ=0.0603 rad (The grey colour represents yielded regions)

## 5 Discussion

A comparison of the measured and FE simulated results for the single-sided shear tabs and the double-sided shear tabs demonstrated that the expected failure mode is different for the two configurations. Figure 15a shows a free body cut for selected sections of the shear plate. This method of evaluation was employed to examine the different load transfer mechanisms in single and double-sided shear tabs. Using these free body cuts, the location of the inflection point was determined (Fig. 15b) and its distance to the centreline of the girder web, i.e. the effective eccentricity ($e_{eff}$), and the centroid of the bolt group, i.e. the bolt group eccentricity ($e_b$), were calculated. The results of the free body cuts are presented and discussed in Sections 5.1 and 5.2.

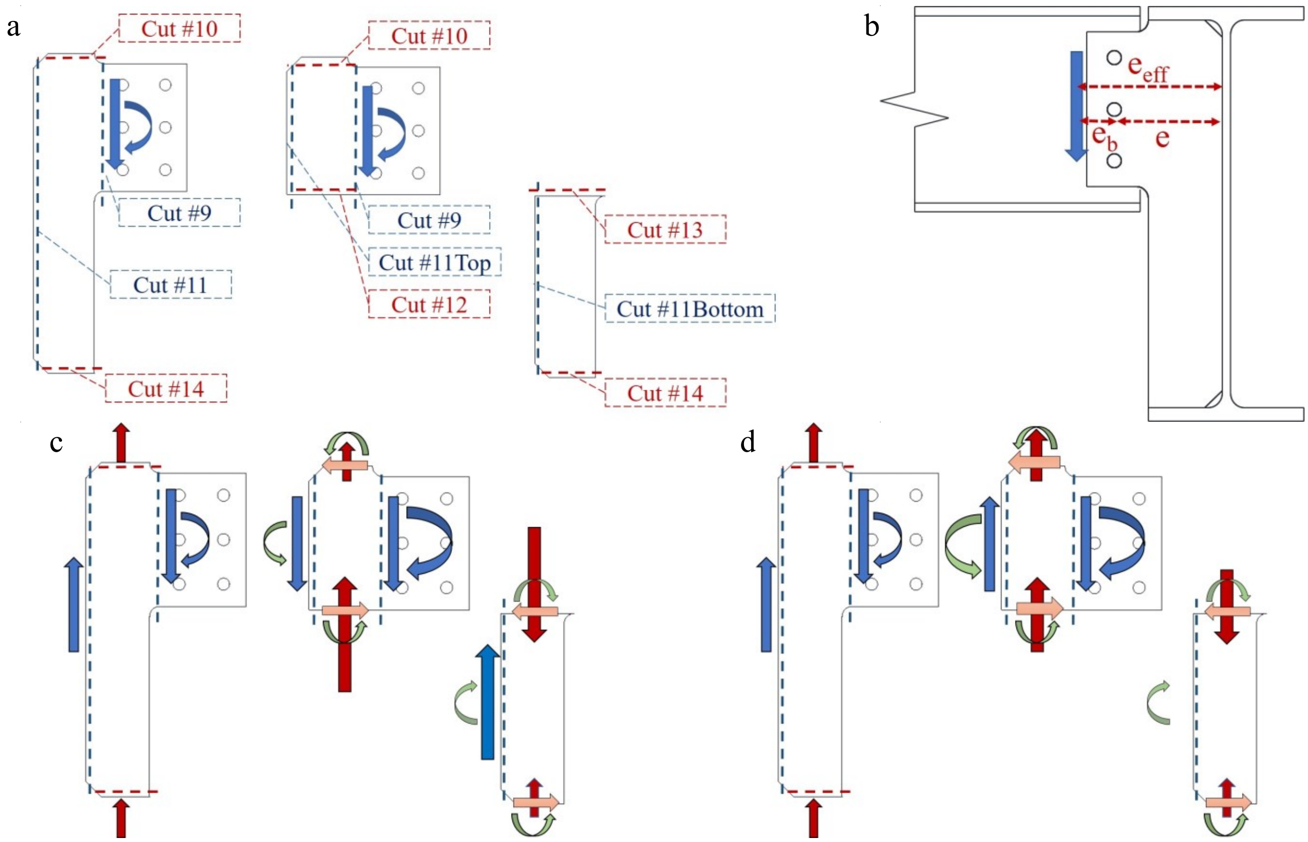


Fig. 15: Free body cuts from FE models (a) defined sections for Free body cuts, (b) connection eccentricity, (c) freebody diagram of single-sided shear tab, (d) freebody diagram of double-sided shear tab

## 5.1 Load transfer mechanism

Figures 16a and 16c show that the compressive axial force, which developed in the stiffened portion of the shear tab (Cut #12), was larger than the connection shear force of the single-sided shear tabs. In contrast, this compressive axial force was smaller than the connection shear force in the double-sided shear tabs (Figs. 16b and 16d). For the FE-E models of shear tab connections BG3-2-10-F and BG3-2-13-F, the ratio between the stiffener axial force and the connection shear force was 1.67 and 0.48 for single-sided and double-sided shear tabs, respectively. As these ratios remained constant for both the slender and compact shear tabs, it can be concluded that they result from the different loading transfer mechanisms for single and double-sided shear tabs.

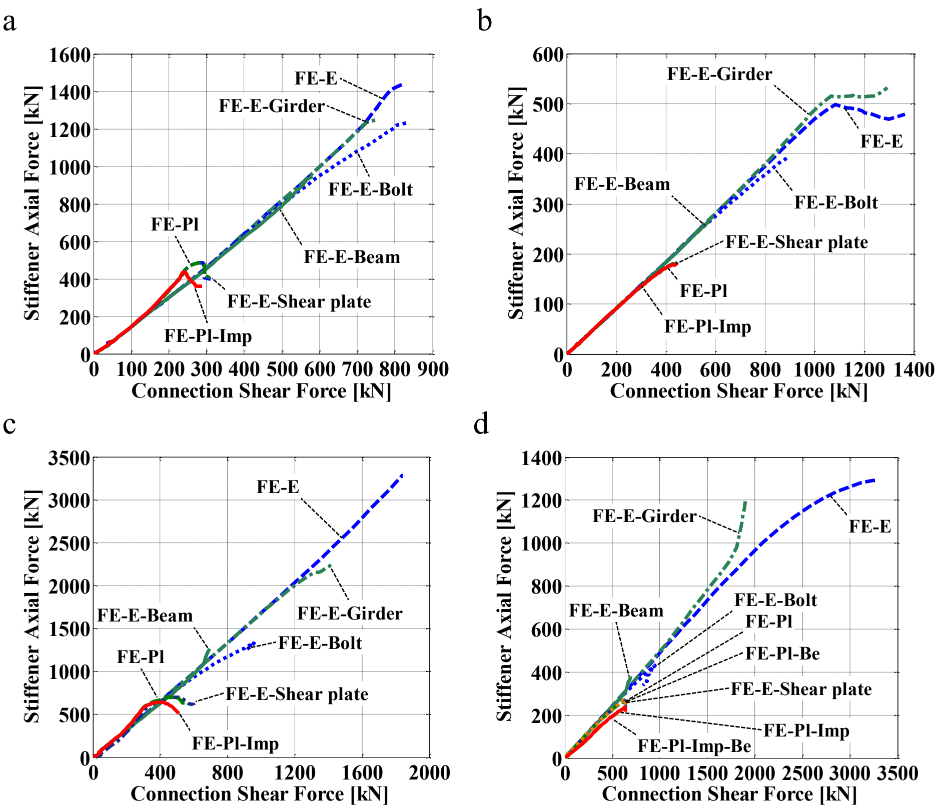


Fig. 16. Predictions of the developed axial force at the stiffener versus the connection shear force for: (a) single-sided configuration of BG3-2-10-F, (b) double-sided configuration of BG3-2-10-F, (c) single-sided configuration of BG3-2-13-F, (d) double-sided configuration of BG3-2-13-F

In order to determine the load transfer mechanism, the forces, developed through different portions of the shear plate, were also studied. Regarding the elastic models of BG3-2-10-F (including single-sided and double-sided), the vertical forces at the shear plate are presented versus the beam rotation in Fig. 17. A large component of the connection shear force of single-sided shear tabs (i.e. Cut #9) was transferred to the girder web (i.e. Cut #11) as a shear force, while the girder flanges (Cut #10 and Cut #14) carried 20% of the connection shear.

Notably, the shear force was not distributed uniformly over the girder web depth, which contradicts the assumptions made in the design procedure of the shear tab connection. Referring to Figs. 15c and 17c, the shear force at the top part of the stiffener (Cut #11Top) developed in the downward direction to counterbalance the moment, mobilized due to the existing eccentricity of the external shear force. Further, horizontal forces developed at the stiffener, along the edges of the extended portion of the shear plate, to counterbalance the bending moment applied to the shear plate at Cut #9 (Fig. 15c). Referring to Fig. 17c, the slope of the curve representing the axial force of the stiffener decreased significantly at 1129 kN compression, which corresponds to a connection shear force equal to 672 kN (0.0375 rad).

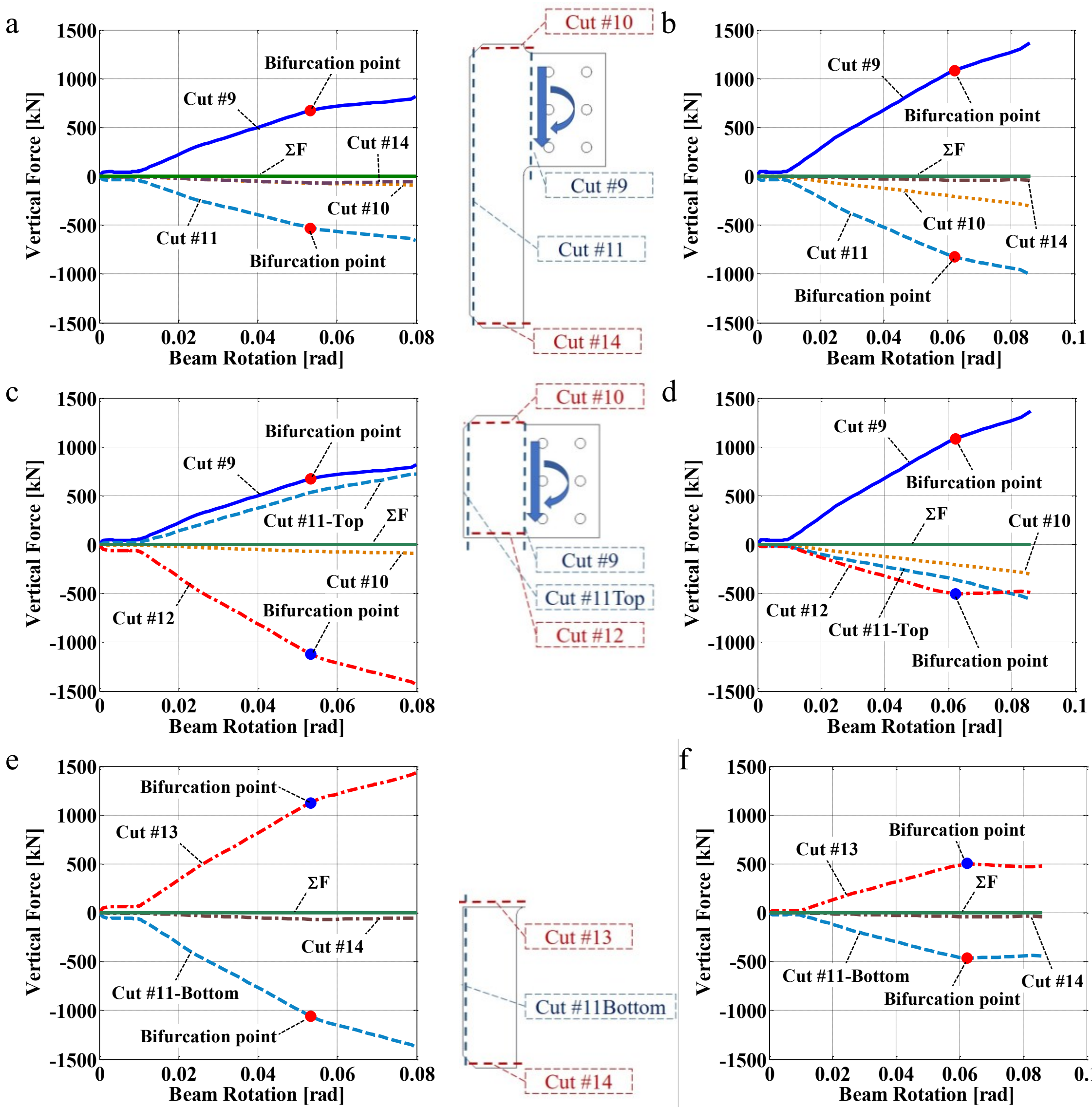


Fig. 17. Prediction of elastic FE models of BG3-2-10-F for vertical force at: (a) stiffener of single-sided connection, b) stiffener of double-sided connection, (c) top part of the stiffener of single-sided connection, (d) top part of the stiffener of double-sided connection, (e) bottom portion of the stiffener of single-sided connection, (f) bottom portion of the stiffener of double-sided connection

Referring to Figs. 15d and 17d, unlike the single-sided shear tabs, the shear force that was developed at the top portion of the stiffener (Cut #11Top) of the double-sided shear tabs was an upwards force that counterbalanced a significant portion of the connection shear force; therefore, the stiffener was subjected to a lower compression force although the double-sided connection was subjected to a higher level of applied shear force in comparison to the single-sided shear tab. The shear tab buckled at 508 kN compression force, which is half the buckling force observed in the single-sided shear tab. This is due to the larger horizontal shear stress along the bottom re-entrant corner of the connection. The horizontal shear stress was mobilized in the stiffener because of the bending moment that developed in the shear tab connection. Due to the higher stiffness of the double-sided shear tab, its inflection point formed farther from the girder as compared to the single-sided shear tab. The upward shear force along Cut #11-Top and the applied shear force along the Cut#9 formed a shear force couple, which caused an extra moment on the stiffener that was counterbalanced by the horizontal force developed in the stiffener. Therefore, the stiffener of the double-sided shear tab was subjected to a much higher horizontal shear stress as compared to the single-sided shear tab. The top flange of the girder resisted 20% of the connection shear force, while the bottom flange negligibly contributed to transfer the connection shear force.

Note that the yielding of the shear plate affected the load transfer mechanism. In single-sided shear tabs, the stiffened portion of the shear plate yielded locally in advance of its elastic buckling. This local yielding resulted in the application of a transverse force to the girder web, which was resisted by out-of-plane bending. Yielding occurred due to the limited out-of-plane bending capacity of the girder web, which resulted in the formation of the girder web mechanism. Comparisons between the results of the single-sided connections illustrated the shear plate's susceptibility to inelastic buckling when the compactness limit for stiffeners was not met. The slender stiffener (BG3-2-10-F) became unstable and reached its strength plateau as soon as it yielded locally, while the compact stiffener (BG3-2-13-F) reached a higher shear force after the local yielding of the shear plate, which is a stable failure mechanism.

The yielding of the shear plate along the net section of the vertical row of bolts, closest to the girder, was observed as the governing failure mode for double-sided shear tabs. The observed strength of double-sided shear tabs for configurations BG3-2-10-F and BG3-2-13-F (430 kN and 630 kN, respectively) was close to the predictions for the rupture of their shear plate at the net section (496 kN and 654 kN for BG3-2-10-F and BG3-2-13-F, respectively). Notably, after yielding along the bolt line, yielding propagated to the stiffener of BG3-2-10-F, and its out-of-plane deformation started to increase. This observation demonstrates that inelastic buckling of the stiffener may also occur in double-sided configurations; which prevents the connection from reaching the shear force corresponding to rupture along the net section.

### 5.2 Effective eccentricity

Based on the shear force and bending moment developed in the shear plate and the bolt group, the location of the inflection point was determined. To calculate the connection eccentricity ($e_{eff} = M/V$), the bending moment and shear force at the outer ends of the re-entrant corners of the shear plate were determined directly using the Free body option available in Abaqus. Figure 18 illustrates the distance between the inflection point and the centroid of the girder web, i.e. the effective eccentricity ($e_{eff}$ in Fig. 15b), for the various connection configurations. In contrast to the current design assumption, the inflection point forms away from the girder web, beyond the centre of the bolt group (Fig. 18); which means $e \leq e_{eff}$. As shown, the shear plate buckling, yielding of the shear plate, yielding of bolts, and the girder web yielding decreased the connection's stiffness and pushed the inflection point toward the girder. The only exception to this observed trend is the FE-E-G model of the double-sided configuration of BG3-2-13-F, for which the shear force reached the girder's shear yielding capacity. Comparisons between the single and double-sided configurations of BG3-2-10-F (Figs. 18a and 18b) and BG3-2-13-F (Figs. 18c and 18d) demonstrated the larger eccentricity of the double-sided configuration at the same level of shear force. This observation can be attributed to the higher stiffness of the double-sided configuration in comparison with the single-sided one. Moreover, the implementation of a thicker shear tab plate for BG3-2-13-F resulted in a higher stiffness and a larger eccentricity under the same level of shear force.

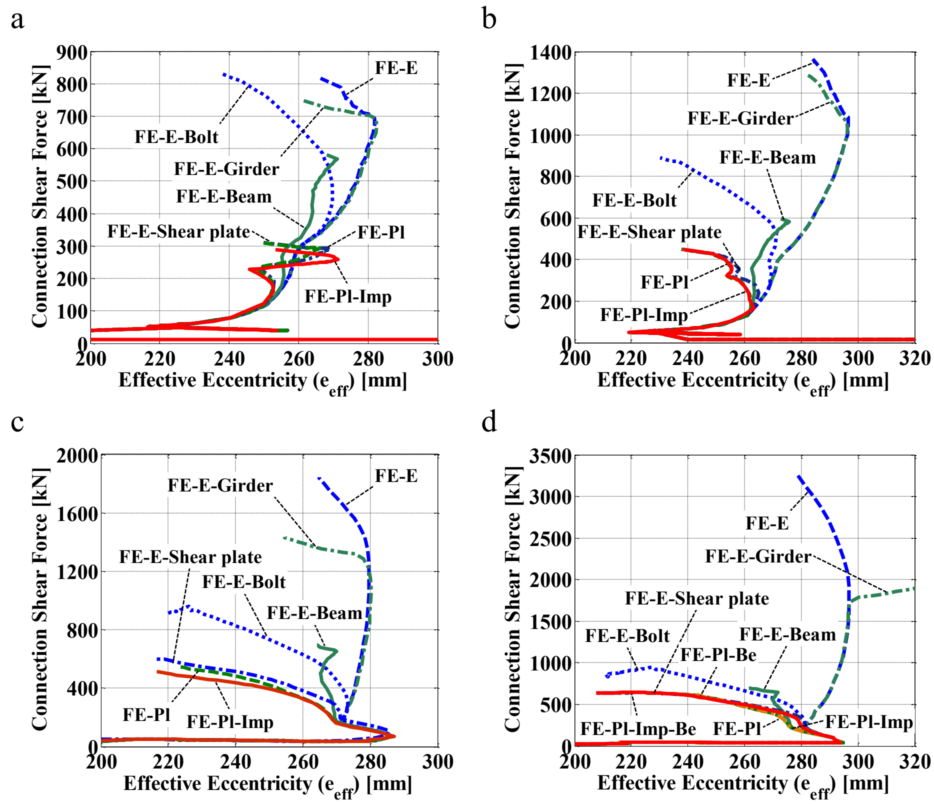


Fig. 18. Predictions of numerical models for shear force versus effective eccentricity at: (a) single-sided configuration of BG3-2-10-F, (b) double-sided configuration of BG3-2-10-F, (c) single-sided configuration of BG3-2-13-F, (d) Double-sided configuration of BG3-2-13-F

The comparison between predictions of the model with a yieldable bolt group (FE-E-Bo) and the model with the yieldable components (FE-Pl) demonstrated that the shear strength of the bolt group was much higher than the shear capacity of the connection. The FE model prediction was compared with available bolt shear experiments [37, 38] in order to ensure the capability of the FE model to detect accurately the bolt shear strength. Although the FE model accurately captured the bolt's strength plateau (continuous increase of the bolt deformation while the bolt force remained constant) in the shear test, it was not possible to capture the bolt's post ultimate (softening) response. This may result in concern regarding the capability of the FE model to capture the shear capacity of the bolt group under an eccentric shear force, in which the bolts would experience shear fracture progressively. To address this issue, the force-deformation response of each individual bolt was monitored during the analysis; the minimum level of the connection shear force corresponding to the time when the first bolt reached its strength plateau was considered as the shear capacity of the bolt group.

Furthermore, as shown in Table 3, the observed bolt shear strength of models FE-E-Bo was much higher than the AISC predictions based on the instantaneous centre of rotation (ICR) method. This over-strength can be attributed to the eccentricity of the bolt group ($e_b$ distance in Fig. 15b) being much smaller than the AISC recommendation for eccentricity ($e$ distance in Fig 15b). This observation mirrored the nature of the AISC method as it relies on the lower bound theorem [7] to provide a conservative, straight forward, and simple to use method for the design of extended shear tabs. However, the AISC Design Manual allows for an alternative bolt group eccentricity consideration if justified by rational analysis [1]. Based on these observations, the bolt shear strength of the connection could be determined based on the bolt group eccentricity ($e_b$) that is equal to the distance between the location of the inflection point and the centre of the bolt group. Notably, the observed bolt group eccentricity should not be extended to a configuration with a different bolt pattern; previous research [27] has demonstrated that the connection eccentricity is a function of the bolt pattern depth. Further studies are needed to propose an equation for the bolt group eccentricity.

Table 3-Bolt shear strength based on predictions of the model FE-E-Bo

| Specimen | FE Model | | Current design eccentricity | | | Revised eccentricity [a] | | |
|---|---|---|---|---|---|---|---|---|
| | Inflection point [b] (mm) | $V_u$ Shear Strength (kN) | Eccentricity (mm) | $V_{SH}$ Shear Strength (kN) | $\frac{V_u}{V_{SH}}$ | Bolt Group Eccentricity (mm) | $V_{SH}$ Shear Strength (kN) | $\frac{V_u}{V_{SH}}$ |
| BG3-2-10-F–S.S [c] | 252 | 709 | 197 | 270 | 2.63 | 49 | 667 | 1.06 |
| BG3-2-10-F–D.S [d] | 251 | 718 | 197 | 270 | 2.66 | 48 | 672 | 1.07 |
| BG3-2-13-F–S.S [c] | 258 | 674 | 197 | 270 | 2.50 | 55 | 641 | 1.05 |
| BG3-2-13-F–D.S [d] | 259 | 670 | 197 | 270 | 2.48 | 56 | 637 | 1.05 |

[a] Based on the observed eccentricity in the model FE-E-Bo
[b] Distance between the location of inflection point and the centre of girder web
[c] Suffix S.S refers to single-sided configuration
[d] Suffix D.S refers to double-sided configuration

As shown in Table 3, this revised definition of the bolt group eccentricity resulted in a reasonably conservative prediction of the bolt shear strength of the connection (the ratio between FE result and prediction based on the revised eccentricity was between 1.05 and 1.07). The smaller ratio between the FE and the analytical predictions for BG3-2-13-F was attributed to the fact that the thicker shear plate provided higher rotational stiffness and the inflection point formed farther from the bolt group centre in comparison to the specimen with the more slender shear tab (BG3-210-F).

Furthermore, the experimentally measured strength of the single-sided BG3-2-13-F (520 kN) was much larger than the design strength, which was based on the shear failure of the bolt group calculated using the instantaneous centre of rotation analysis method with the eccentricity equal to the distance between the centre of the bolt group and the weld line (270 kN), i.e. as per the current practicing design method. This observation further validated the prediction of the FE models with respect to the formation of the inflection point along the exterior bolt line.

## 6 Conclusions

Owing to the lack of a comprehensive published procedure for the design of stiffened extended shear tab connections, practicing engineers often use the current AISC design procedure, even though it was originally developed for unstiffened extended shear tabs. This method assumes that the inflection point forms at the face of the supporting girder or column and that the weld attachment between the shear plate and the girder flanges (i.e., stabilizer plates) is ignored. Experiments on stiffened extended shear tabs have demonstrated that these weld attachments influence the load transfer mechanism within the connection. Therefore, there is concern with respect to the validity of the aforementioned design assumptions.

To better understand the behaviour of stiffened extended shear tabs (full-depth stiffeners), full-scale laboratory tests and complementary finite element simulations were conducted. This paper contains a summary of the finite element studies of two beam-to-girder shear tab configurations. The numerical models were validated with previously conducted full-scale experiments on representative connections. The main findings of the corroborating FE study are summarized as follows:

- The inflection point of extended beam-to-girder shear tabs with full depth shear plates is away from the girder centreline (i.e. beyond the centre of the bolt group) in both the single- and double-sided configurations. Hence, the current practice for design of these connections may not be always conservative as it underestimates the force demands on the stiffened portion of the shear tab as well as the bending demands on the supporting element.
- The stiffened portion of extended beam-to-girder shear tabs with full-depth shear plates (including single-sided and double-sided configurations) is subjected to vertical axial and horizontal shear forces simultaneously. This is not considered in the current design procedure. The axial and shear force demands are strongly dependent on the out-of-plane stiffness of the girder web and the connection eccentricity.

- Single-sided extended beam-to-girder shear tabs with full-depth shear plate experience yielding in their stiffened portion along the bottom re-entrant corner. Out-of-plane deformations tend to increase in such case.
- Single-sided extended beam-to-girder shear tabs with full-depth shear plates experience shear forces much higher than those anticipated based on design values representative of shear failure of the bolt group. This is an indication that the bolt group eccentricity may be significantly smaller than the assumed value, i.e. the distance between the weld line and the centre of the bolt group.
- The ultimate shear capacity of the bolt group can be determined by calculation on the basis of the bolt group eccentricity, the distance between the inflection point and the centre of the bolt group. For the studied bolt pattern (i.e., two vertical lines of three bolts), the inflection point formed beyond the vertical bolt line, farthest from the girder. Of note, this location is not representative of connections with different bolt pattern because the location of the inflection points is a function of the bolt pattern depth. Additional studies are necessary to develop an empirical equation for the bolt group eccentricity.
- In the absence of a robust method to predict the buckling strength of the stiffened portion of the shear plate, the local buckling failure mode of the shear plate should be considered. The use of shear plates that satisfy the CSA S16 compactness ratio for stiffeners ( $200/\sqrt{F_y}$ ) results in a stable shear tab connection behaviour.
- The behaviour of double-sided extended beam-to-girder shear tabs with full-depth shear plates differs from that of single-sided connections. In comparison to the single-sided connections, a much lower compressive force develops in the stiffener of a double-sided connection while the connection is subjected to a higher shear force. In advance of yielding

of the stiffened portion of the shear plate, these connections experience shear plate yielding at the net section of the vertical row of bolts, closest to the girder.

To extend this research to the point where recommendations for design can be made a numerical parametric study is needed to validate the observations described herein for a greater range of stiffened extended shear tab connections. This work is ongoing.

## 7 Acknowledgments

The authors would like to thank the ADF Group Inc. and DPHV Structural Consultants for their generous technical and financial support, as well as the Natural Sciences and Engineering Research Council of Canada. The authors also thank Jacob Hertz and Nathan Goldstein Apt for sharing their experimental results for extended shear tabs. The finite element computations were conducted on the McGill University supercomputer Guillimin, which is managed by Calcul Québec and Compute Canada. The supercomputer operation is funded by the Canada Foundation for Innovation (CFI), NanoQuébec, RMGA and the Fonds de recherche du Québec - Nature et technologies (FRQ-NT).

## 8 References

[1] AISC 325-17, Steel Construction Manual, 15$^{th}$ edition, American Institute of steel Construction, Chicago, IL, 2017. (Chapter 7: pp.6-8, Chapter 9: pp.6-10, Chapter 10: pp.87-91 & 127-132)

[2] AISC 360-16, Specification for Structural Steel Buildings, American Institute of Steel Construction, Chicago, IL, 2016.

[3] B. Dowswell, R. Whyte, Local stability of double-coped beams, Eng. J. AISC, 51(1) (2014), pp. 43–51.

[4] AISC 325-11, Steel Construction Manual, 14$^{th}$ edition, American Institute of steel Construction, Chicago, IL, 2011. (Chapter 9: pp.6-10)

[5] J.J. Cheng, J.A. Yura, C.F. Johnson, Design and behavior of coped beams, University of Texas at Austin, Austin, TX, 1984.

[6] L.S. Muir, W.A. Thornton, Direct method for obtaining plate buckling coefficient for double coped beams , Eng. J. AISC, 41 (3) (2004), pp. 133–134.

[7] L.S. Muir, C.M. Hewitt, Design of unstiffened extended single-plate shear connections, Eng. J. AISC, 46 (2) (2009), pp. 67-79.

[8].W.A. Thornton, P.J. Fortney, On the need for stiffeners for and the effect of lap eccentricity on extended single-plate connections, Eng. J. AISC, 48(2) (2011),pp. 117-125.

[9] A. Elkady, D.G. Lignos, Full-scale testing of deep wide-flange steel columns under multiaxis cyclic loading: loading sequence, boundary effects, and lateral stability bracing force demands, J. Struct. Eng. ASCE, 144 (2) (2018), 04017189.

[10] D.R. Sherman, A. Ghorbanpoor, Design of extended shear tabs, University of Wisconsin-Milwaukee, Milwaukee, WI, 2002.

[11] W. Goodrich, Behavior of extended shear tabs in stiffened beam-to-column web connections," M.Sc. Thesis, Vanderbilt University, Nashville, TN, 2005.

[12] K. Thomas, R.G. Driver, S.A. Oosterhof,, L. Callele, Full-scale tests of stabilized and unstabilized extended single-plate connections, Structures, 10 (2017), pp.49-58.

[13] M. Mahamid, A. Rahman, A. Ghorbanpoor, The analyses of extended shear tab steel connections part II: stiffened connections, Eng. J. AISC, 44 (2) (2007), pp. 133-146.

[14] P.J. Fortney, W.A. Thornton, Analysis and design of stabilizer plates in single-plate shear connections, Eng. J. AISC, 53 (1) (2016), pp. 1-28.

[15] M. Marosi, Behaviour of single and double row bolted shear tab connections and weld retrofits," Master's Thesis, McGill University, Montreal, QC, 2011.

[16] M. Marosi, M. D'Aronco, R. Tremblay, C.A. Rogers, Multi-row bolted beam-to-column shear tab connections, 6th European Conference on Steel and Composite Structures, Budapest (2011).

[17] M. D'Aronco, Behaviour of double and triple vertical rows of bolts shear tab connections and weld retrofits," Master's Thesis, École Polytechnique de Montréal, Montreal, QC, 2013.

[18] A. Mirzaei, Steel shear tab connections subjected to combined shear and axial forces, PhD Thesis, McGill University, Montreal, QC, 2014.

[19] J. Hertz, Testing of extended shear tab connections subjected to shear, Master's Thesis, McGill University, Montreal, QC, 2014.

[20] N. Goldstein Apt, Testing of extended shear tab and coped beam-to-girder connections subject to shear loading, Master's Thesis, McGill University, Montreal, QC, 2015.

[21] J. Hertz, D.G. Lignos, C.A. Rogers, Full scale testing of extended beam-to-column and Beam-to-girder shear tab connections subjected to shear, 8th International Conference on Behavior of Steel Structures in Seismic Areas, Shanghai (2015).

[22] C.A. Rogers, Marosi M., Hertz J., Lignos D., Tremblay R., D'Aronco M., Performance of weld-retrofit beam-to-column shear tab connections, Connections VIII, 8th International Workshop on Connections in Steel Structures, Boston, MA ( 2016).

[23] CSA-S16-14, Limit States Design of Steel Structures, Canadian Standards Association, Toronto, ON, 2014.

[24] ASTM A992 / A992M-11(2015), Standard Specification for Structural Steel Shapes, ASTM International, West Conshohocken, PA, 2015.

[25] ASTM A572 / A572M-15, Standard Specification for High-Strength Low-Alloy Columbium-Vanadium Structural Steel, ASTM International, West Conshohocken, PA, 2015.

[26] ASTM F3125 / F3125M-15a, Standard Specification for High Strength Structural Bolts, Steel and Alloy Steel, Heat Treated, 120 ksi (830 MPa) and 150 ksi (1040 MPa) Minimum Tensile Strength, Inch and Metric Dimensions, ASTM International, West Conshohocken, PA, 2015.

[27] A. Astaneh-Asl, K.M. McMullin, S.M. Call, Behavior and design of steel single plate shear connections, J. Struct. Eng. ASCE, 119 (8) (1993), pp. 2421-2440.

[28] AISC 341-16, Seismic Provisions for Structural Steel Buildings, American Institute of Steel Construction, Chicago, IL, 2016.

[29] ABAQUS 6.11-3, [Computer software], Dassault Systemes Simulia Corp., Providence, RI.

[30] G.L. Kulak, J.W. Fisher, H.A. Struik, Guide to design criteria for bolted and riveted joints, 2nd Edition. American Institute of Steel Construction, Chicago, IL, 2001.

[31] I.R. Gomez, A.M. Kanvinde, Y.K. Kwan, G.Y. Grondin,Strength and ductility of fillet welds subjected to out of plane bending, American Institute of Steel Construction, Chicago, IL, 2008.

[32] ASTM A6/A6M-04b, Standard specification for general requirements for rolled structural steel bars, plates, shapes, and sheet piling, American Society for Testing and Materials, West Conshohocken, PA, 2004.

[33] CSA-G40.20-13/G40.21-13, General requirements for rolled or welded structural quality steel/ structural quality steel, Canadian Standards Association, Toronto, ON, 2013.

[34] CISC, Handbook of steel construction, 11th edition, Canadian Institute of Steel Construction, Markham, ON, 2016.

[35] A. Elkady, D.G. Lignos, Analytical investigation of the cyclic behavior and plastic hinge formation in deep wide-flange steel beam-columns, Bull. Earthq. Eng., 13 (4) (2015), pp. 1097-1118.

[36] H. Daneshvar, One-sided steel shear connections in column removal scenario," PhD. Thesis, University of Alberta, Edmonton, AL, 2013.

[37] J.J Wallaert, J.W. Fisher, The shear strength of high-strength bolts, Lehigh University, Bethlehem, PA,1964.

[38] J.J Wallaert, J.W. Fisher. Shear strength of high-strength bolts, J. Struct. Div. ASCE, 91 (3) (1965), pp. 99-126.